

# Intervertebral disc degeneration affects the distribution of internal stresses and strains within human lumbar vertebrae

K.A. Raftery<sup>1a</sup>, A. Kargarzadeh<sup>1</sup>, S. Tavana<sup>1</sup>, and N. Newell<sup>1</sup>

<sup>1</sup>Department of Bioengineering, Imperial College London, London, UK

<sup>a</sup>kay.raftery18@imperial.ac.uk

## Introduction

Vertebral compression fractures are the most prevalent type of osteoporotic fracture [1]. However, use of bone mineral density (BMD) to predict strength is inadequate, as up to 50% of post-menopausal women suffering fractures are not osteoporotic [2]. It has been shown *in vitro* that loading vertebrae through the adjacent intervertebral discs (IVDs) causes strains near the endplate region to increase by up to 132% relative to directly loading the vertebra without IVDs [3]. However, the effect of common IVD pathologies such as disc degeneration on the internal strain distribution of the vertebra is unknown. Better understanding of how the IVD contributes to vertebral fracture susceptibility could lead to the utilisation of disc degeneration metrics in routine fracture assessment.

Trabecular strains can be measured using digital volume correlation (DVC) [4]. However, quantification of internal stress distributions *in vitro* has not yet been attempted, which could provide crucial information regarding the mechanical state of the vertebra. Therefore, the aims of this study were to i) use DVC to evaluate the implications of disc degeneration on vertebral trabecular strains; ii) establish a novel pipeline for quantifying trabecular von Mises stress; and iii) explore correlations between disc degeneration, bone morphology (BMD, trabecular architecture), and bone mechanics (strain, stress).

## Methods

**Specimen preparation:** Six human cadaveric lumbar spines (48±13 years, Table 1) were obtained after approval from the Imperial College Tissue Bank Ethics Committee. Specimens were dissected to remove all soft tissue, ligaments, and facet joints, sectioned into bi-segments (Fig. 1A), and potted in polymethylmethacrylate. Prepared specimens were kept frozen at -20°C prior to testing.

**Clinical imaging:** Specimens were imaged with quantitative-CT (0.98x0.98x0.6mm voxel size) to calculate volumetric BMD (vBMD) using a hydroxyapatite phantom. vBMD was then converted to Young's modulus [5] on a per-voxel basis. To quantify disc degeneration, cranial and caudal Pfirrmann grades [6] of each specimen were evaluated by three independent reviewers on T2-weighted 3T MRIs (KR, AZ, NN). Samples were divided into two groups based on their average Pfirrmann grade: "degenerated" (average Pfirrmann grade > 2, N=3) and "non-degenerated" (average Pfirrmann grade ≤ 2, N=3) (Table 1).

Specimen #	Level	Age	Gender	Caudal Pfirrmann	Cranial Pfirrmann	Average Pfirrmann	Group
1	L4	39	M	2	3	2.5	D
2	L4	64	M	2	2	2	ND
3	L4	60	M	4	5	4.5	D
4	L5	29	F	1	3	2	ND
5	L5	46	F	2	3	2.5	D
6	L5	50	F	2	2	2	ND

Table 1 – Sample demographics. Level refers to the middle vertebra in the segment. D = degenerated IVDs, ND = non-degenerated IVDs

**Biomechanical testing & DVC protocol:**  $\mu$ CT images (140kVp, 10W, 39 $\mu$ m<sup>3</sup> voxel size) were acquired of each specimen in the unloaded (50N axial compression) and loaded (1000N) state. Load was applied using a universal testing machine, and held at the resultant displacement by tightening nuts on a bespoke compression rig (Fig.1A). DVC was performed in DaVis (v10.2, LaVision, Germany). A fast-Fourier transform + direct correlation approach was used, with a final subset size of 38 voxel and 0% subset overlap. A zero-strain study demonstrated that the accuracy and precision of the pooled strain tensor components using this subset size was 386.4 $\mu\epsilon$  and 296.8 $\mu\epsilon$ , respectively.

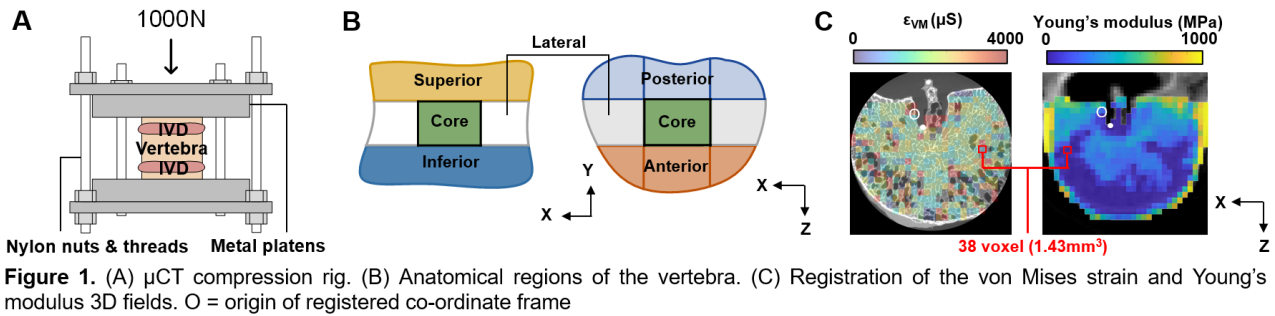
**Analysis:** The unloaded  $\mu$ CT image for each specimen was used to calculate trabecular thickness and separation. 3D strain, BMD, and trabecular microarchitecture fields were imported into MATLAB to calculate mean values within six anatomical regions (Fig.1B). To convert DVC-derived strains into stresses, the von Mises strain ( $\epsilon_{VM}$ ) was calculated as a function of the 3D strain tensor components ( $\epsilon_{xx}$ ,  $\epsilon_{yy}$ ,  $\epsilon_{zz}$ ) (Eq.1):

$$\epsilon_{VM} = 2/3 \sqrt{(3/2 (\epsilon_{xx}^2 + \epsilon_{yy}^2 + \epsilon_{zz}^2) - \epsilon_{xx}\epsilon_{yy} - \epsilon_{xx}\epsilon_{zz} - \epsilon_{yy}\epsilon_{zz} + 3 (\epsilon_{xy}^2 + \epsilon_{xz}^2 + \epsilon_{yz}^2))} \quad (1)$$

A custom-written MATLAB script registered the trabecular Young's modulus and von Mises strain fields together (Fig.1C), and then calculated von Mises stress for all subsets with co-ordinates (i,j,k), under the assumption of a linear, isotropic, and elastic material (Eq.2):

$$\sigma_{VM(i,j,k)} = E_{QCT(i,j,k)} \epsilon_{VM(i,j,k)} \quad (2)$$

To investigate the effect of disc degeneration on endplate stress, the von Mises stress distributions in the superior and inferior regions adjacent to degenerated (N=5) and non-degenerated (N=7) IVDs were compared.



## Results

Specimens with degenerated IVDs displayed significantly lower compressive axial strains ( $-502 \pm 80 \mu\text{S}$ ,  $p < 0.0001$ ), minimum principal strains ( $-697.9 \pm 130 \mu\text{S}$ ,  $p < 0.01$ ), and higher maximum shear strains ( $+507.5 \pm 144 \mu\text{S}$ ,  $p < 0.01$ ) relative to non-degenerated. The anterior region contributed the most to this difference ( $+87.8\%$  averaged across strain types,  $p < 0.05$ ), alongside the superior and inferior regions ( $p < 0.05$ ) (Fig.2A,B). In these regions, trabecular separation was significantly higher when IVDs were degenerated ( $p < 0.05$ ) (Fig.2C). Average Pfirrmann grade significantly and positively correlated with the compressive axial and minimum principal strain ratio between the endplate (superior and inferior) region relative to the core ( $\rho = 0.93$ ,  $p < 0.05$ ). Von Mises stresses were similar in both groups (D:  $0.45 \pm 0.13 \text{MPa}$ , ND:  $0.57 \pm 0.22 \text{MPa}$ ) ( $p < 0.26$ ) (Fig.2D). However, stresses in the endplate regions adjacent to non-degenerated IVDs peaked in the core region, whilst this peak was shifted to the anterior region when adjacent to degenerated IVDs (Fig.2E,F).

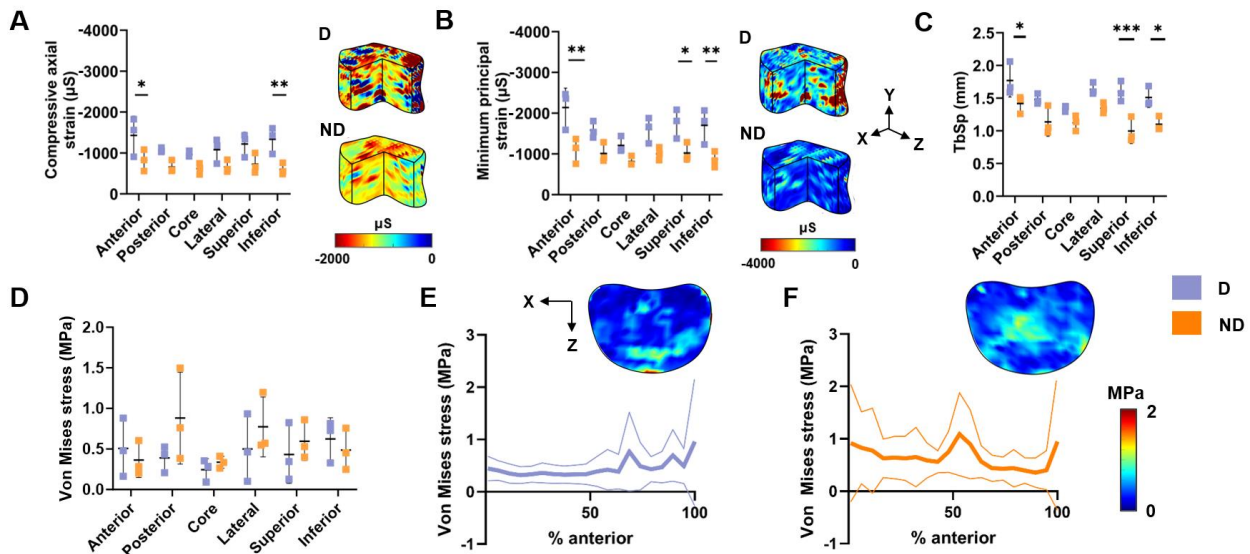


**Figure 2.** (A) Compressive axial strains, (B) minimum principal strains, (C) trabecular separation (TbSp) and (D) von Mises stress per anatomical region. 3D compressive and minimum principal strain fields are shown for a typical specimen in each group. \*\*\* $p < 0.001$ , \*\* $p < 0.01$ , \* $p < 0.05$ . (E,F) Anteroposterior von Mises stress distribution in the endplate regions underlying (E) degenerated and (F) non-degenerated IVDs. For each group, a typical mid-transverse map of the von Mises stress is shown. D = degenerated, ND = non-degenerated.

## Conclusion

Disc degeneration is associated with increased strains in the anterior, superior, and inferior regions of the vertebra, which may increase vulnerability to endplate or anterior-wedge compression fracture. Von Mises stress magnitudes were influenced by disc degeneration to a lesser degree. However, stress peaks occurred in the central endplate region only in vertebrae with non-degenerated IVDs, highlighting the importance of load transfer through the central pressurised region when the IVDs are healthy, possibly preventing bone reabsorption at the adjacent endplate regions. This study supports the notion that metrics of IVD morphology could enhance fracture risk prediction.

## References

- [1] R. Burge et al. *J Bone Miner Res.* Vol. 22 (2007)
- [2] K.M. Sanders et al. *Bone.* Vol. 38 (2006)
- [3] A.I. Hussein et al. *J Biomech.* Vol. 46 (2013)
- [4] A.I. Hussein et al. *Procedia IUTAM.* Vol. 4 (2012)
- [5] D.L. Kopperdahl et al. *J Orthop Res.* Vol. 20 (2002)
- [6] C.W.A. Pfirrmann et al. *Spine.* Vol. 26 (2001)